Torres Górriz, B.; Bertolesi, E.; Calderón García, PA.; Moragues, JJ.; Adam, JM. (15-0). A full-scale timbrel cross vault subjected to vertical cyclical displacements in one of its supports. Engineering Structures. 183:791-804. https://doi.org/10.1016/j.engstruct.2019.01.054

A Full-scale Timbrel Cross Vault Subjected to Vertical Cyclical Displacements in One of its Supports

Benjamín Torres, Elisa Bertolesi*, Pedro A. Calderón, Juan J. Moragues, Jose M. Adam

ICITECH, Universitat Politècnica de València. Camino de Vera s/n, 46022 Valencia, Spain

Abstract

Up-and-down cyclical displacement of supports-foundations, due for example to the presence of expansive soils, can affect the integrity of a structure and may even lead to its collapse. A recent study carried out at the ICITECH laboratories of the *Universitat Politècnica de València* analysed the effects of earth settlements on the behaviour of masonry cross vaults. One of the tests involved the construction and testing of a full-scale timbrel cross vault, one of whose supports was subjected to up-and-down vertical displacement cycles. The 4×4 m^2 vault was composed of four 3.6 m diameter arches supporting a masonry web. Vertical displacements were applied to one of the supports by means of two synchronised mechanical jacks. The results of the tests provide valuable information to the scientific community, architects and engineers on the behaviour of timbrel cross vaults when one of their supports is subjected to cyclical movements.

Keywords

Cross vault; Settlement; Masonry; Experimental test; Full-scale; Vertical cyclical displacement

* Corresponding author. Tel.: +39 3496597648

E-mail address: elber4@upv.es (E. Bertolesi).

1. Introduction

Masonry cross vaults have been used for centuries with a covering function in many historical buildings such as churches and palaces. They are characterized by their own particular architectural features, such as ribs, groins and masonry webs [1].

The experimental results of extensive *in-situ* surveys of the damage frequently encountered in masonry cross vaults have shown that the surroundings in which the structure is placed can play a critical role. This has led to a change in the focus of the scientific community: if the context has a dominant influence on structural performance, the structural behaviour cannot be evaluated in isolation, but must be considered within its context [1][2][3][4][5]. Although it is difficult to take into account all the effects of the surrounding structures when analysing structural performance, identifying the causes of recurring cracking patterns can detect possible failure scenarios and undiscovered vulnerable aspects and might suggest additional and effective safety-oriented retrofitting strategies [6][5].

Several studies have focused on the damage patterns in failures of masonry cross vaults. The information obtained from *in-situ* surveys helps to identify possible structural deficiencies and to propose new interventions for their rehabilitation [7][8]. These analyses are able to provide invaluable information on the behaviour of cross vaults within the context of their surroundings. This type of analysis has been used in important case studies, such as the collapse of the cross vault in the Basilica of St. Francis of Assisi (Italy) [9]. However, the information collected in such cases is usually specific to the case study at hand and can only be partially generalized. A simplification of the phenomenon is sometimes obtained in laboratory experiments, in which a selected set of external actions is applied to a masonry structure and its effects evaluated in relation to the capacity of the structure and the damage patterns found.

As full-scale experimental investigations are difficult and expensive to carry out, most studies are conducted on scaled-down prototypes, as for example in the work of Theodossopoulos et al. [7][8], who analysed the behaviour of a prototype based on one of the ribbed quadripartite vaults in the Abbey Church of Holyrood (Edinburgh) subjected to the horizontal movement of two supports. The

experimental study aimed at identifying the collapse mechanism responsible for the displacement of the perimeter walls and a formation of the well-known Sabouret cracks.

Another example of a laboratory campaign carried out on a scaled-down prototype with dry joints was carried out in [10], which included a series of experimental tests of different movements of the supports and evaluating the evolution of the crack patterns at failure for each support configuration. When a vertical movement was applied to the prototype, both relative displacements of the blocks near the support and sliding along the diagonal affected the structure causing its collapse. Although horizontal displacement produced an arch mechanism with the formation of three alternate hinges, the collapse of the vault was caused by relative sliding problems between the blocks close to the support. During the diagonal collapse test, the activation of an arch mechanism was detected at three alternate hinges. The results of the numerical and experimental investigations confirmed the adaptive capacity of the vault to find an equilibrium in conditions of serious instability.

The effect of different sets of movements of the supports was applied to scaled down cross vault in [11][12]. In [11] a 1:5 scale cross vault was loaded by means of a tilting plane test.

The results of the experimental campaign showed the formation of a four-hinge mechanism in the vault‘s webs and the development of a typical diagonal crack on the top of the vault when a shear deformation was applied to the prototype. Furthermore, a significant non-linear and ductile response was obtained at the end of the test. When a cyclic displacement was applied, the results underlined evidently dissipative behaviour characterized by maximum strengths similar to those obtained from the monotonic tests. A longitudinal opening mechanism caused the formation of a three-hinge symmetric mechanism in the two webs subjected to opening, whereas in the longitudinal closing mechanism the vault showed a high capacity for deformation. The strength was equal to 15 % of the total weight of the structure.

In most of the works cited, the effect of vertical or horizontal displacements on the behaviour of cross vaults is assessed by simplified methods.

The development of 3D printers has now reduced the cost of lab tests on dry-joint masonry vaults. Tests have been conducted on masonry prototypes divided into an arbitrary number of blocks, which are assembled manually to obtain the final structure. The number of bricks constitutes the first limitation,

as cracks and displacements can only occur along the lines of the dry interfaces, so that the number of blocks in the structure plays a crucial role in terms of the collapse behaviour actually found. The second limitation involves the manual assembly of the blocks, which can introduce different types of defects and lead to premature collapse and underestimation of the vault's displacement capacity. In addition, in real full-scale structures, the mortar distributes the contact pressures and avoids stress concentrations. These limitations mean that the experimental testing of full-scale masonry cross vaults is required to understand and analyse in detail the behaviour of this type of structure, especially when cyclic settlements are applied.

Another important limitation of the cited studies is the limited number of external distortions analysed. Most of these works consider the effect of horizontal movements of the supports and few focus on the influence of vertical movements on the overall behaviour of masonry vaults, while even fewer deal with the effect of cyclic earth settlements [13][14]. This latter phenomenon is particularly interesting from a technical point of view because of its strong influence on the behaviour of masonry structures and on cross vaults in particular. The most important causes of soil settlements are: expansive soils, surrounding excavations and variations in soil humidity. Examples of differential foundation settlements include the settlement of buildings in Venice caused by soft soils [15], the Cathedral of Agrigento [16] and the Milan Duomo [17].The first example is very specific to the Venetian lagoon environment. Indeed, in that case the ground stratigraphy, characterized by limited bearing capacity and compressibility, played a crucial role and influenced the typology of building constructed in that area. Agrigento Cathedral represents an important example of how slope instability problems can affect the structural behaviour of masonry constructions, while Milan Duomo suffered the effects of subsidence problems [18].

In general, a combination of cyclic settlements is more critical for buildings than other types of soil movements. Masonry structures built on expansive soils are frequently subjected to severe distortions on certain types of ground. The most common results of soil movements are the development of cracks and damage, which can compromise a building's normal structural functioning and stability [19].

The present work is intended to follow this line of research on masonry structures with an innovative and unique experimental analysis of the behaviour of a masonry cross vault subjected to an

upward/downward vertical settlement. This cross vault is square in shape with dimensions of 4x4 m^2 and its lateral arches are 1.8 m high. Cyclic settlement was applied to one of the vault supports by means of two mechanical jacks. The crack patterns and collapse mechanisms were monitored during the test bya purpose-built monitoring system consisting of 23 sensors, including LVDTs and Fibre Optic sensors.No experimental studies in the technical literature deal with full-scale masonry structures. As this is probably the first time that a full-scale masonry cross vault has been subjected to a simulated soil settlement, the results are expected to be of great interest to the scientific community, practitioners and stakeholders working in this field.

The paper is structured in five parts as follows: in Section 2 the main features of the case study are described, including the experimental set-up, data acquisition equipment, the numerical model used, and the mechanical properties of the masonry materials. Section 3 describes the construction of the full-scale vault, and the experimental results are presented in Section 4. Section 5 gives a detailed description of the experimental output in terms of the cracking patterns identified and the structural behaviour of the vault.

2. Case study

The study carried out in the ICITECH laboratories of the *Universitat Politecnica de Valencia* (Spain) involved a full-scale masonry cross vault subjected to a series of cyclic settlements on one of its supports. The study was based on the vaults in the Church of San Lorenzo de Castell de Cabres (Castellón, Spain) [20], in which some vaults had been damaged by a downward displacement of their supports. In fact, a visual inspection of the church revealed the presence of various cracks on the surface of the masonry webs and one vault had partially collapsed with the loss of almost half of its webbing, as shown in Figure 1. The crack patterns detected during the *in-situ* surveys suggested the partial collapse of the vault had been due to soil settlements [20].

According to [21], masonry cross vaults are prone to damage and premature collapse mostly because of distortions in the supports, which can be produced by horizontal displacements of the perimeter walls or by a vertical soil settlements. To study the effects of this latter phenomenon, a vault geometrically similar to the one partially collapsed in the Church of San Lorenzo de Castell de Cabres was constructed

in the laboratory with slight variations in the position of the supports to adapt to the lab conditions. It is worth mentioning that, due to the impossibility of defining the real boundary conditions of the vaults in the Church of San Lorenzo de Castell de Cabres as well as the effect of the building's overall rigidity, the collapse inspired the construction of a test vault with respect to the geometry and the construction technique only. In fact, the aim of the present investigation was to analyse one of the most serious sources of damage to masonry vaults, derive their displacement capacity and identify their damage mechanisms. The vault supports were placed at the corners of a 4x4 m square with four 3.6 m diameter semi-circular lateral arches. The arches were approximately 1.8 m high and the total height of the structure plus the concrete base and the test apparatus reached 2.51 m.

The arches comprised four layers of bricks and three layers of mortar. The brick dimensions were 230x110x26 mm^3. The vault rested on four steel supports, labelled S1, S2, S3 and S4, the series of settlement cycles being applied to S1. Except for support S3, which was completely fixed, the others were designed to allow monitoring of the vertical reaction forces during the construction and testing of the vault. Particular attention was paid to the mechanism used to apply the vertical displacement, which allowed the application of cyclical vertical movements and free perpendicular and horizontal displacements. The vertical settlements were applied by two mechanical jacks fixed to a 20 mm thick steel plate. The synchronised quasi-static movements were applied manually to avoid undesired rotations, allowing visual inspection of the vault and the identification of damage patterns during the test. Unlike support S1, S2 and S4 could only move horizontally.

a

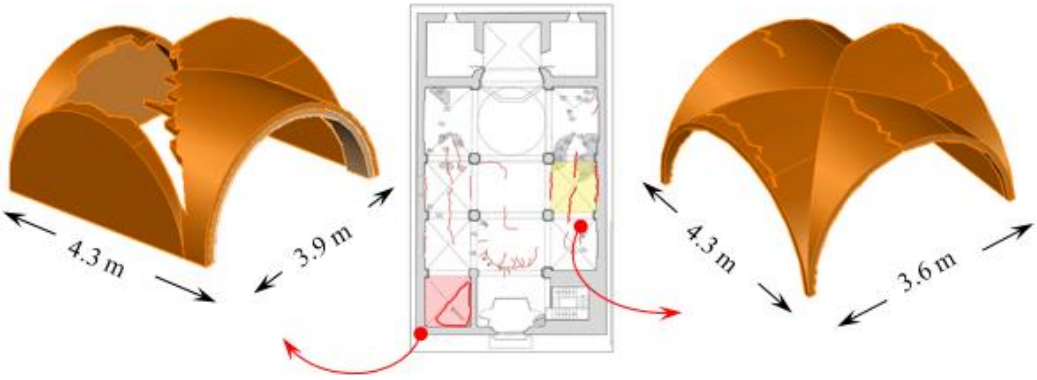

b

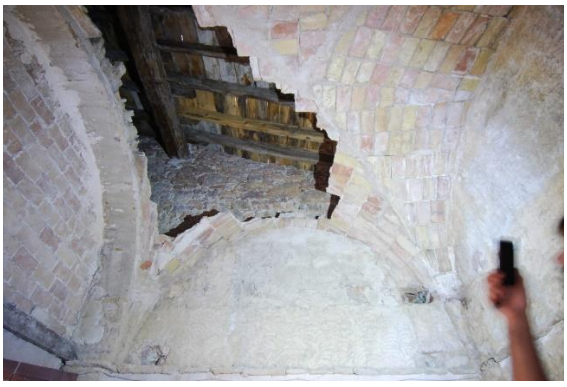

Figure 1: Church of San Lorenzo de Castell de Cabres (Spain): geometry of the damaged vaults (a) and failure mechanism of one of the vaults (b).

The steel devices adopted are shown in Figure 2. A steel cylinder with a diameter of 159 mm and height of 200 mm, fixed to a steel box, was placed on supports S1, S2 and S3. Three strain gauges were attached to the supports at approximately mid-height to monitor the reaction forces. The steel box was composed of two sections connected by ball bearings 20 mm in diameter. The bearings were designed to reduce friction and provide a smooth sliding contact between the two steel surfaces.

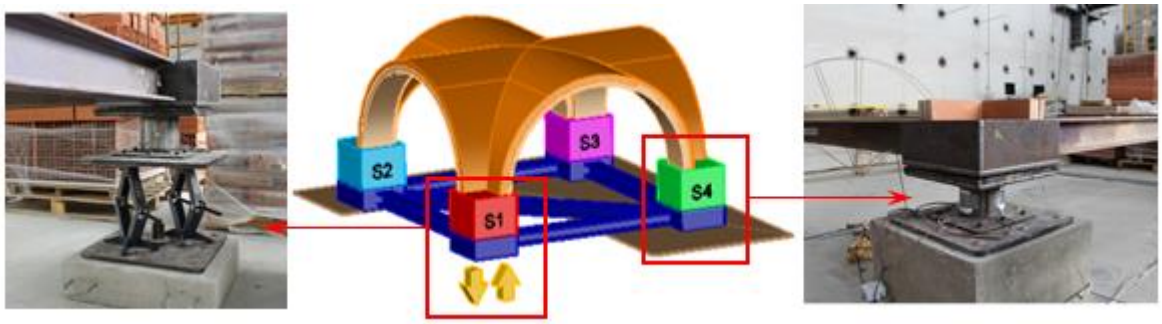

Figure 2: Experimental set-up: steel mechanisms adopted to allow the horizontal and vertical displacements of the vault supports.

As can be seen in Figure 2, a 600x600x500 mm^3 reinforced concrete cube was used to anchor the vault supports to the mechanical system. The concrete cubes were reinforced by 12 mm diameter horizontal and vertical steel bars. Each steel base was connected by a steel bracing system composed of 140 mm steel girders welded to the bases in such a way as to allow axial loads only (see Figure 2). The aim of the bracing system was twofold: (i) to prevent the premature failure of the cross vault during the testdue to possible horizontal displacements of the supports and (ii) to mimic the partial lateral constraints furnished by the presence of adjoining vaulting systems.

2.1 Numerical model

During the design phase of the experimental set-up, some analyses were conducted by means of an isotropic elastic FE model on LUSAS software [22] for the preliminary assessment of the vault behaviour when subjected to a monotonically increasing downward settlement. The results of the numerical model were used to evaluate an upper bound of: (i) the vertical reaction forces in each support, (ii) the areas of the vault where the maximum stresses were expected to occur and (iii) the axial loads on the steel bracing system. Given the complexity of the cross vault tested, it was only possible to develop an elastic FE model of the vault during the design phase.

A 3D FE elastic model was built with four-node shell elements for the masonry webs and arches. The concrete supports were simulated by means of hexahedral FEs and the steel frame used to connect the supports was modelled with 2-nodes trusses. It’s worth mentioning that due to the adopted construction technique (the vault has been constructed with two layer overlapped perpendicularly and with mortar

materials having similar elastic properties), its orthotropic behavior vanishes and therefore it was neglected in the proposed analyses. The vault prototype was loaded with its own self-weight and was then subjected to a vertical settlement of support S1. The mechanical properties adopted for the masonry, steel and concrete supports are summarized in Table 1, with the specific weights of the materials involved in the analyses. The elastic moduli of the masonry and concrete were defined from the results of tests on both materials. The steel elastic modulus was assumed to be as furnished by its manufacturer.

Material	**Young Modulus E [MPa]**	**Poisson ratio, υ [-]**	**Density, ρ [kN/m^3]**
Masonry	2100	0.2	18
Concrete	30000	0.2	20
Steel (beams)	209000	0.3	78

Table 1: Mechanical properties of the materials adopted in the FE model.

The numerical predictions confirmed the need for the steel bracing system. When a vertical displacement was applied to one of the vault supports, there were horizontal displacements in both S2 and S4. It appeared clear that without a steel frame as a lateral partial constraint, S2 and S4 would have been forced to move diagonally outwards, which could easily have led to a premature failure of the vault itself. In addition, these movements are generally associated with a diagonal distortion of the vault, which is out of the scope of the present paper. According to [6], diagonal distortions are characterized by a different failure mechanism than that involved in the vaults in the Church of San Lorenzo de Castell de Cabres. It is worth mentioning that, cross vaults are rarely constructed as isolated elements, and were frequently adopted in the past to span lateral and central church naves. This means that these vaults are often inserted between adjoining vaulting systems and thick perimeter walls. which prevent free movements of the vault supports.

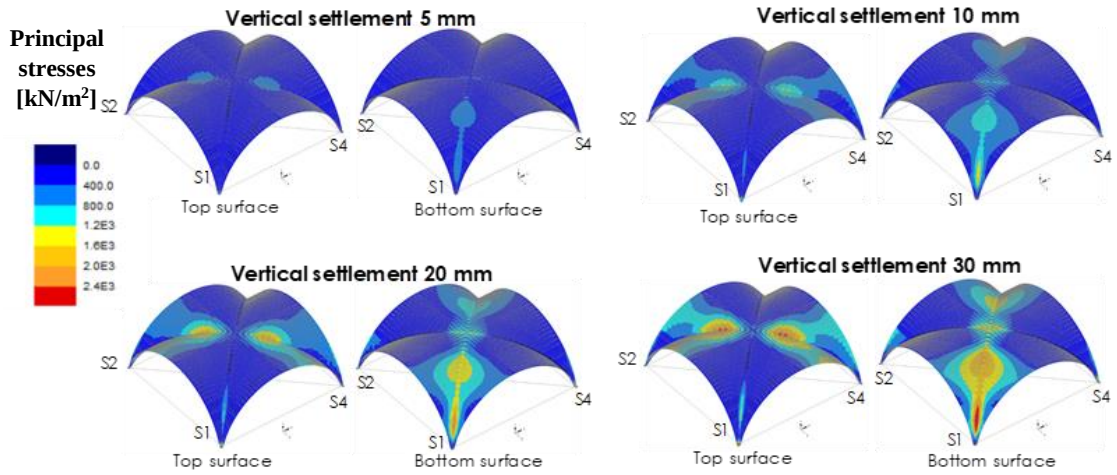

Figure 3: Numerical results obtained from the FE elastic model: tensile principal stresses at different values of imposed displacement.

The FE model guided the definition of the steel bracing system. The axial loads on the steel frame obtained numerically were used to design the steel girders used in the bracing. Meaningful information was obtained from the distribution of the principal stresses along the vault. The tensile stresses reached their maximum value on the web extrados along the diagonal elliptic arch S2-S4, which would explain the formation of a diagonal crack along the line connecting supports S2-S4 on the upper face of the vault, while other critical zones were found in the four arches and the web intrados close to S1 and S3 (see Figure 3).

2.2 Mechanical properties of the constituent materials

This section describes the laboratory investigation performed to identify the mechanical properties of the masonry material adopted to construct the cross vault. The timbrel vault and lateral arches were built of clay bricks, two different types of mortar (lime mortar and cement mortar) and plaster paste.

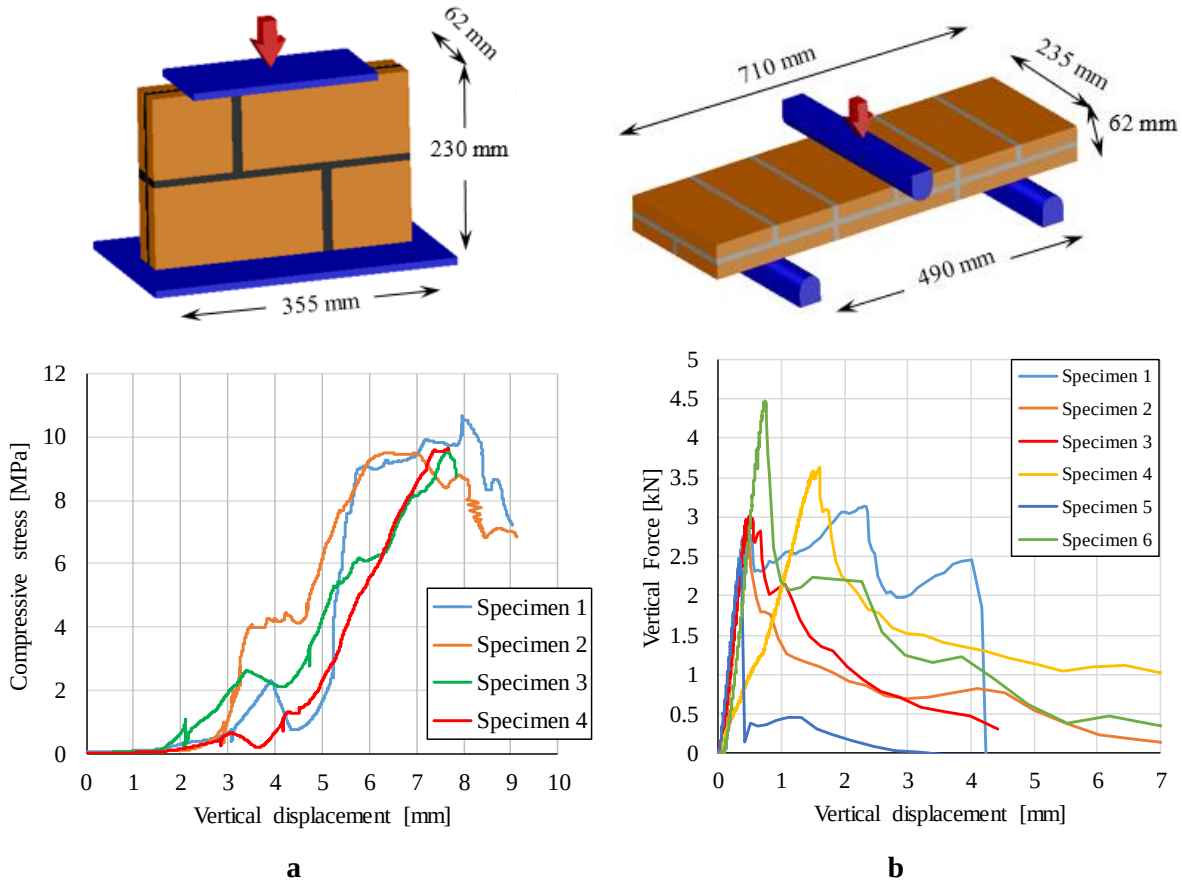

a **b**

Figure 4: Laboratory test set-up and obtained results: compressive test (a) and three-point bending test (b).

The analyses comprised the experimental testing of a total of 10 masonry prisms to identify the mechanical properties of the masonry in the web. Four of the samples were tested under compression and the remainder were tested by a three-point bending test. The two experimental set-ups are depicted in Figure 4, together with the specimen dimensions. The results obtained are shown in Table 2.

Type of test	**Compression test**	
	Compressive strength [MPa]	**Displacement at failure [mm]**
Specimen 1	10.5	8
Specimen 2	9.5	6.5
Specimen 3	9.5	7.5
Specimen 4	9.7	7.5
Average	**9.8**	**7.375**
Type of test	**Three point bending test**	
	Flexural strength [MPa]	
Specimen 1	1.783	
Specimen 2	1.594	
Specimen 3	1.707	
Specimen 4	2.065	
Specimen 5	1.396	
Specimen 6	2.545	
Average	**1.848**	

Table 2: Mechanical properties of the vault masonry.

As can be seen in Table 2, a larger experimental scatter was found in the results of the three-point bending tests, while those of the compressive tests showed higher consistency.

2.3 Experimental set-up and data acquisition

The experimental investigation consisted of the laboratory testing of a full scale timbrel cross vault under the controlled displacement of one of its supports. The cyclic settlement history is depicted in Figure 5. As can be noted, the lab protocol consisted of the application of a series of controlled vertical displacement (downward-upward) cycles, gradually increasing the magnitude of the imposed displacement. Each amplitude was executed by one complete cycle (upward/downward displacement) in which the movement was gradually increased by doubling the vertical displacement applied at the end of the previous one. The experimental test was stopped when the crack widths compromised the stability of the structure. Indeed, after the test, the damaged cross vault was repaired with textile-reinforced mortar (TRM) placed on the extrados surface. The strengthened vault was then re-tested by applying a series of cyclic settlements to support S1 to evaluate the effectiveness of the cement-based materials (TRM/FRCM) for the retrofitting of full-scale masonry cross vaults. The analysis of this test is outside the scope of this paper and will be disseminated in the near future.

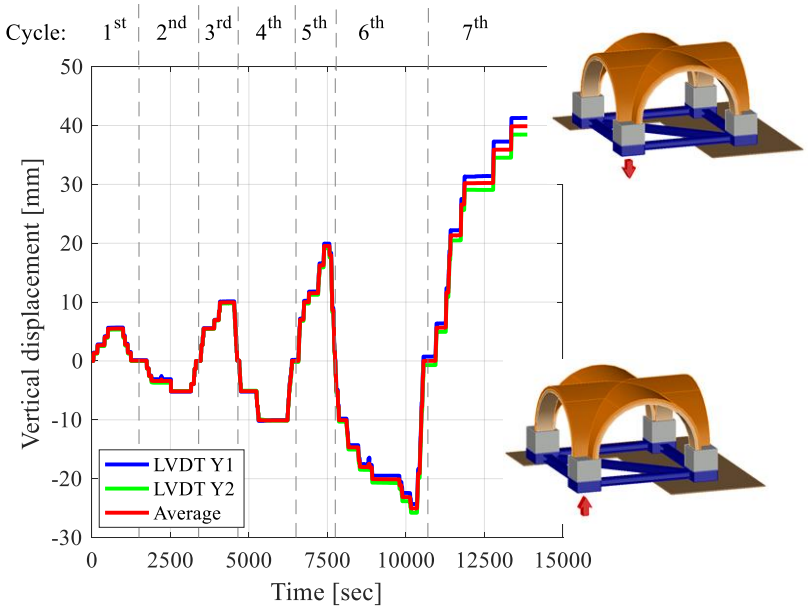

Figure 5: Displacement history of one of the supports of the cross vault tested.

During the experimental test, different parts of the masonry vault were monitored to characterise its structural behaviour by evaluating: (i) the evolution of the reaction forces in the supports, (ii) the widening of cracks and the corresponding changes in vault behaviour, (iii) the history of the displacements applied to support S1, and (iv) the axial loads on the steel bracing system. The vertical reaction forces were evaluated by three strain gauges (-120˚/0˚/120˚) placed on the steel tubes forming the mechanical support system. The value of the vertical forces was calculated from the average deformation recorded by the strain gauges and considering a steel elastic modulus of 210 GPa.

Vault deformation was monitored by two systems: (i) Linear Variable Displacement Transducers (LVDTs) and (ii) Fibre Optic Sensors (FOSs). A summary of the instrumentation used for the test is shown in Table 3, and their positions on the vault are shown in Figure 6. Both LVDTs and FO sensors were placed at points where cracks were expected. The most critical zones were identified from the results obtained by the previously described FE elastic model. Although evaluating crack growth mechanisms is a complex task when a series of cyclic settlements are imposed, the most probable failure mechanism was the separation of the vault along one of the diagonal elliptic arches. To follow the movements applied to the vault, flexural cracks were expected in the lateral arches and tensile cracks near supports S1 and S3. LVDTs 2-5 were used to monitor the arches' behaviour, while most of the other sensors were attached to the upper surface of the vault along the critical diagonal (S2-S4). Only

one sensor (LVDT 3) was positioned on the opposite diagonal elliptic arch (S1-S3). The same procedure was followed for the positioning of the Fibre Optic Sensors [23][24], as shown in Figure 6.

Long gauge sensor	**Length [mm]**	**Location**
LVDT1	640	On support S1, on elliptical arch S1-S3
LVDT2	465	On support S2, on arch S1-S2
LVDT3	630	On support S2, on arch S2-S3
LVDT4	610	On support S3.
LVDT5	640	On support S4, on arch S3-S4.
LVDT6	420	Upper surface of vault on elliptical arch S2-S4
LVDT7	440	Upper surface of vault on elliptical arch S2-S4
FOS1	310	On support S3.
FOS2	310	Upper surface of the vault on elliptical arch S2-S4
FOS3	1000	Upper surface of vault on elliptical arch S2-S4
S1 _X	150	On support S1, horizontally in X direction
S1 _Z	150	On support S1, horizontally in Z direction
S2 _X	150	On support S2, horizontally in X direction
S2 _Z	150	On support S2, horizontally in Z direction
S4 _X	150	On support S4, horizontally in X direction
S4 _Z	150	On support S4, horizontally in Z direction
LVDT_Y1	300	On support S1, vertically in Y direction
LVDT_Y2	300	On support S1, vertically in Y direction

Table 3: Instrumentation used for the experimental study.

Data was acquired by means of two specific systems. The measurements from the strain gauges and Linear Displacement Transducers were collected on CATMAN software (HBM) [25], and the fibre optic sensors were managed by means of MOI ENLIGHT software (Micron Optics) [26].

The axial loads on the steel bracing system were estimated indirectly by five strain gauges placed at the centre of the girder web plates and labelled P1, P2, P3, P4 and P5, as shown in Figure 6-d.

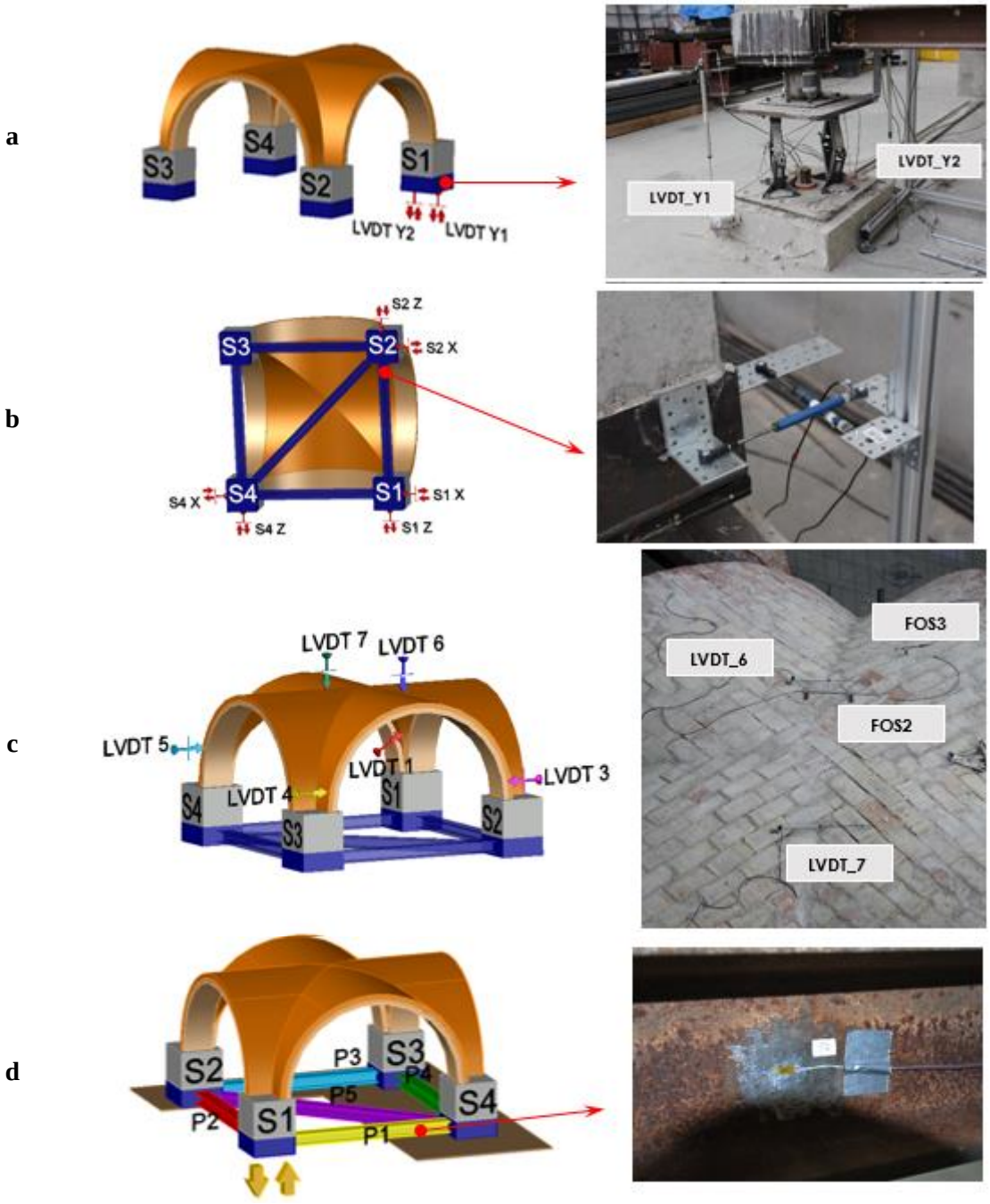

Figure 6: Position of the monitoring apparatus on the vault: vertical LVDTs (a), horizontal LVDTs (b), sensors on the upper vault surface (c) and strain gauges on the steel frame (d).

3. Construction phases

The construction process of the timbrel vault (see Figure 7) involved the following steps:

- Construction of the 1st layer of the four lateral arches using a steel scaffolding system (Figure 7-A);

- Construction of the 2nd layer of the four lateral arches using the arches previously built as scaffolding (Figure 7-B);
- Construction of the 1st layer of the vault webs (Figure 7-C);
- Construction of the 2nd layer of the vault webs (Figure 7-D);
- Repetition of Steps 4-5 laying the bricks towards the centre of the vault (Figure 7-E);
- Covering the central portion of the vault (Figure 7-F)

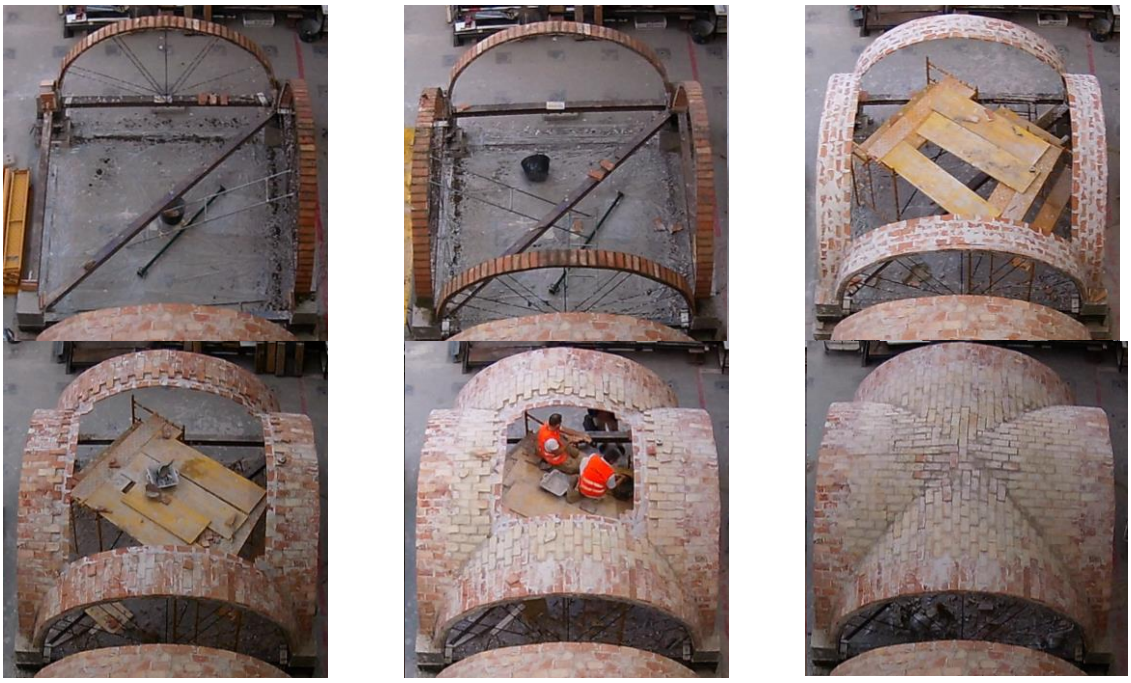

Figure 7: Timbrel vault construction process.

As shown inFigure 7, the lateral arches were built by means of a formwork system positioned on the steel frame as shown in Figure 7-A. The formwork used to construct the first two arches was dismantled after 48 hours and then re-used to build the other two. Figure 8shows a scheme of the layers of bricks and mortar in the four lateral arches, composed of a total of four layers of bricks and three layers of mortar. The arches were approximately 160 mm thick and the mortar joints approximately 10 mm thick.

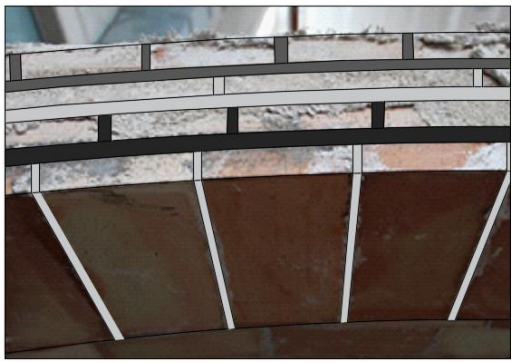

7th	**Vault:** bricks + lime mortar
6th	lime mortar joint
5th	**Vault:** bricks + plaster paste
4th	plaster paste joint
3rd	**Arch:** bricks + cement mortar
2nd	cement mortar joint
1st	**Arch:** bricks + plaster paste

Figure 8: Masonry cross vault: detail of one of the arch.

The webs were built by a special process. The first layer of masonry started from the four lateral arches using the same type of bricks as in the arches plus a plaster paste. When the vault reached a height of approximately 1.5 m, the second layer of the webs was laid diagonally on the first (to improve vault behaviour) with a 10 mm thick layer of lime mortar (see Figure 8). The process was repeated until reaching the intersection of the groins. During this phase the web intrados was completed from underneath the vault and the top layer from above.

During the construction process, the vertical reactions of three of the four supports were constantly monitored. The time evolutions of the vertical forces are given in Figure 9, together with the time steps at which the images shown in Figure 7were extracted. The third support, S3, was completely fixed. Although it was not possible to monitor the vertical reaction at this point, an indirect estimation of the vertical force was obtained by means of the vertical equilibrium of forces of the total weight of the cross vault (35 kN). This value was approximately 9 kN. As can be seen in Figure 9, the vertical forces followed approximately the same trend during the construction process, as was confirmed by the total values of the vertical force on each support at the end of the construction process, which was symmetrically distributed along the four supports and approximately 9 kN. The slight differences found can be explained by several concurring factors, which are always present in experimental tests: the material's heterogeneity, the unsymmetrical geometry induced by the construction process and the masonry texture.

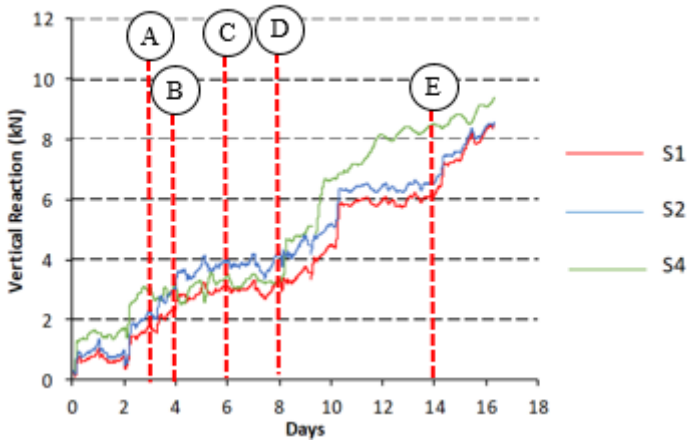

Figure 9: Time evolution of the vertical reactions during the construction.

4. Experimental results

To explore the behaviour of the timbrel cross vault when loaded by a series of cyclic settlements, support S1 was subjected to the displacements depicted in Figure 5. The maximum displacements imposed were equal to 40 mm and -25 mm, considering a downward and upward movement, respectively. The time evolutions of the vertical reactions of all the supports are shown in Figure 10. As expected, the four monitored supports experienced a series of loading-unloading cycles. The distribution of the vertical forces on the four supports is quite symmetric. When a downward displacement was applied to support S1, the loads increased on the two opposite sides (S2 and S4), while S1 and S3 remained unloaded. Conversely, when an upward movement was applied to the vault, the opposite behaviour was observed. This trend could be seen throughout the entire test and even beyond the elastic limit of the vault, as can be seen in Figure 10.

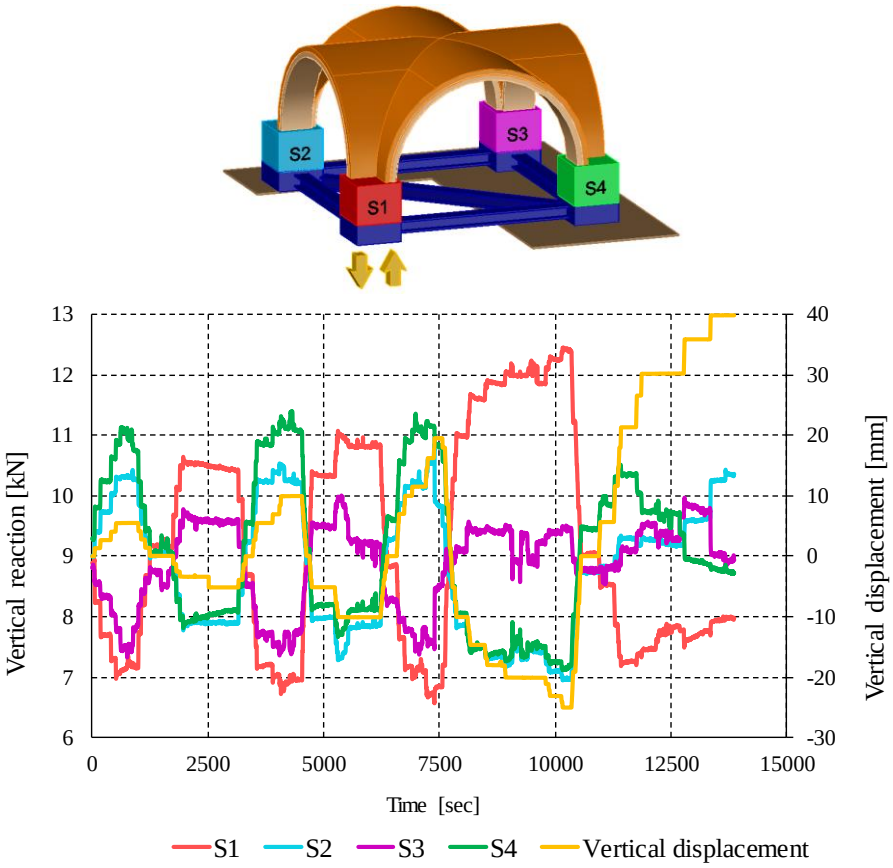

Figure 10: Time evolution of the vertical reactions monitored in the supports.

Similar results were obtained from the strain gauges on the girders of the steel bracing system. Indeed, the evolution of the axial loads measured by the strain gauges followed the trend of the vertical reaction forces obtained in each support. The load-displacement curves obtained in all the monitored supports are given in Figure 11. After the first elastic phase (in the first settlement cycle), significant cracking appeared on the vault which affected its behaviour. This is particularly evident from the beginning of the second cycle in the hysteretic curve by the higher energy dissipation and residual displacements, as showed in Figure 12. Indeed, Figure 12-a shows the degradation of the elastic stiffness of all the supports during the experimental investigation. Elastic stiffness Ke was calculated by considering the secant stiffness of each loading phase at 70% of the maximum force. As expected, the trend of the stiffness degradation during the test was quite similar in all the supports monitored and was not influenced by whether the displacement imposed was downward or upward. In all the cycles, the loops gradually widened and tilted toward the horizontal axis. Stiffness degradation is usually accompanied

by strength degradation in masonry structures. Figure 12-b depicts the ratio between the maximum force recorded in each cycle and the maximum force obtained in the first. As can be noted, this parameter is strongly influenced by the type of displacement imposed. When downward displacements were applied, the maximum force trend was fairly constant throughout the test. In the upward movements, the maximum forces increased in support S1, while in the others gradual degradation was observed. Another important parameter that can be used to understand energy dissipation during the cracking mechanism is the ultimate displacement *Du*. In the present work this was obtained by considering the displacement at the 20% degradation point of the maximum force. The ratio between the ultimate displacement and the elastic one is showed in Figure 12-c.

Supports S2 and S4 showed quite similar behaviour during the whole test, as confirmed by Figure 11-b and –d. Conversely, slightly different results were found in S1 and S3. This asymmetric behaviour was noted not only in the experimental load-displacement curves, but also in the damage patterns at failure. The cracking mechanism is usually strongly influenced by the heterogeneities of the masonry material, which can be present in the vault from the beginning or produced during the experimental test, and by the wide variability in the characteristics of the constituent materials.

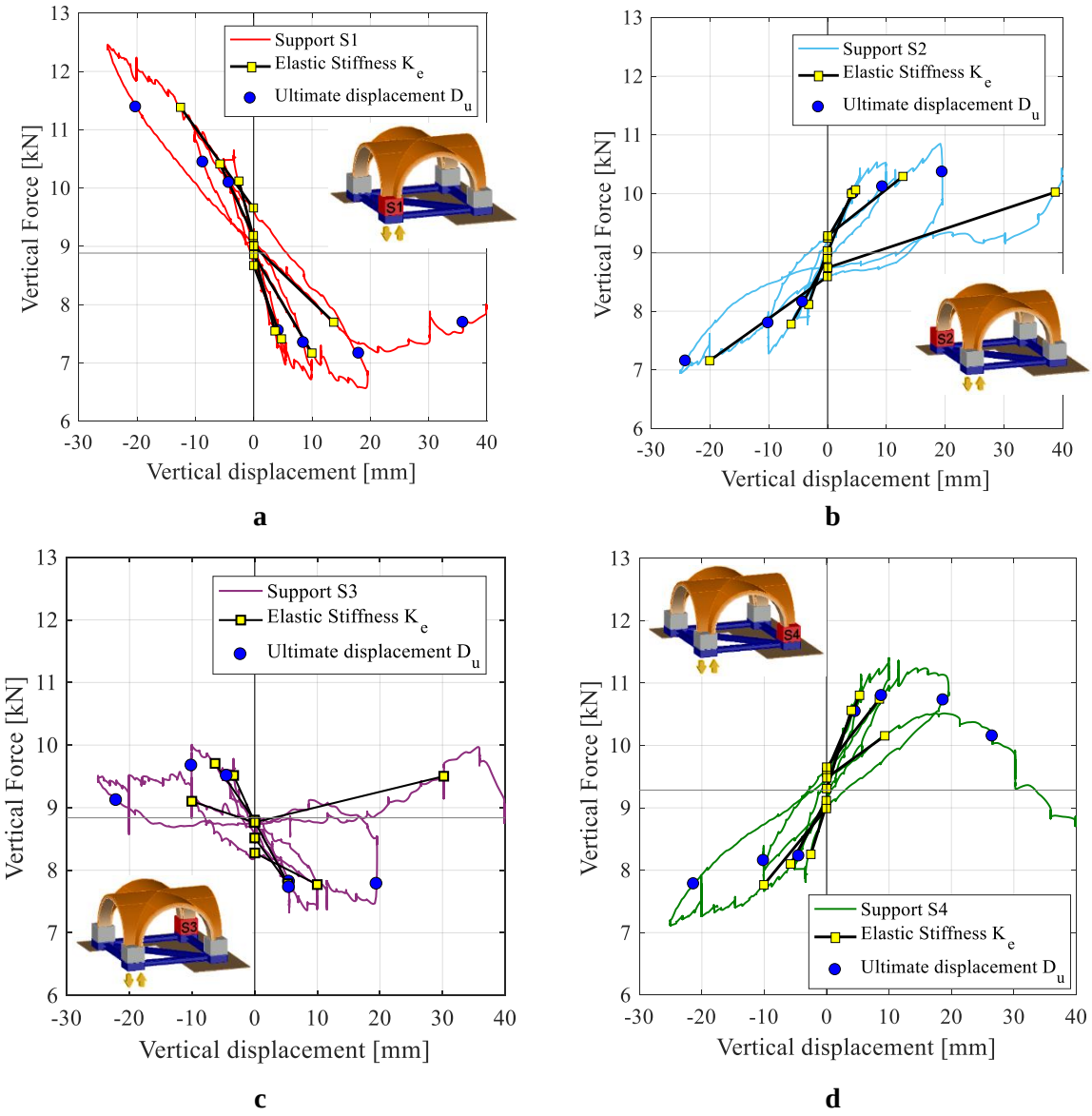

Figure 11: Force-displacement curves in all the abutments: S1 (a), S2 (b), S3 (c) and S4 (d).

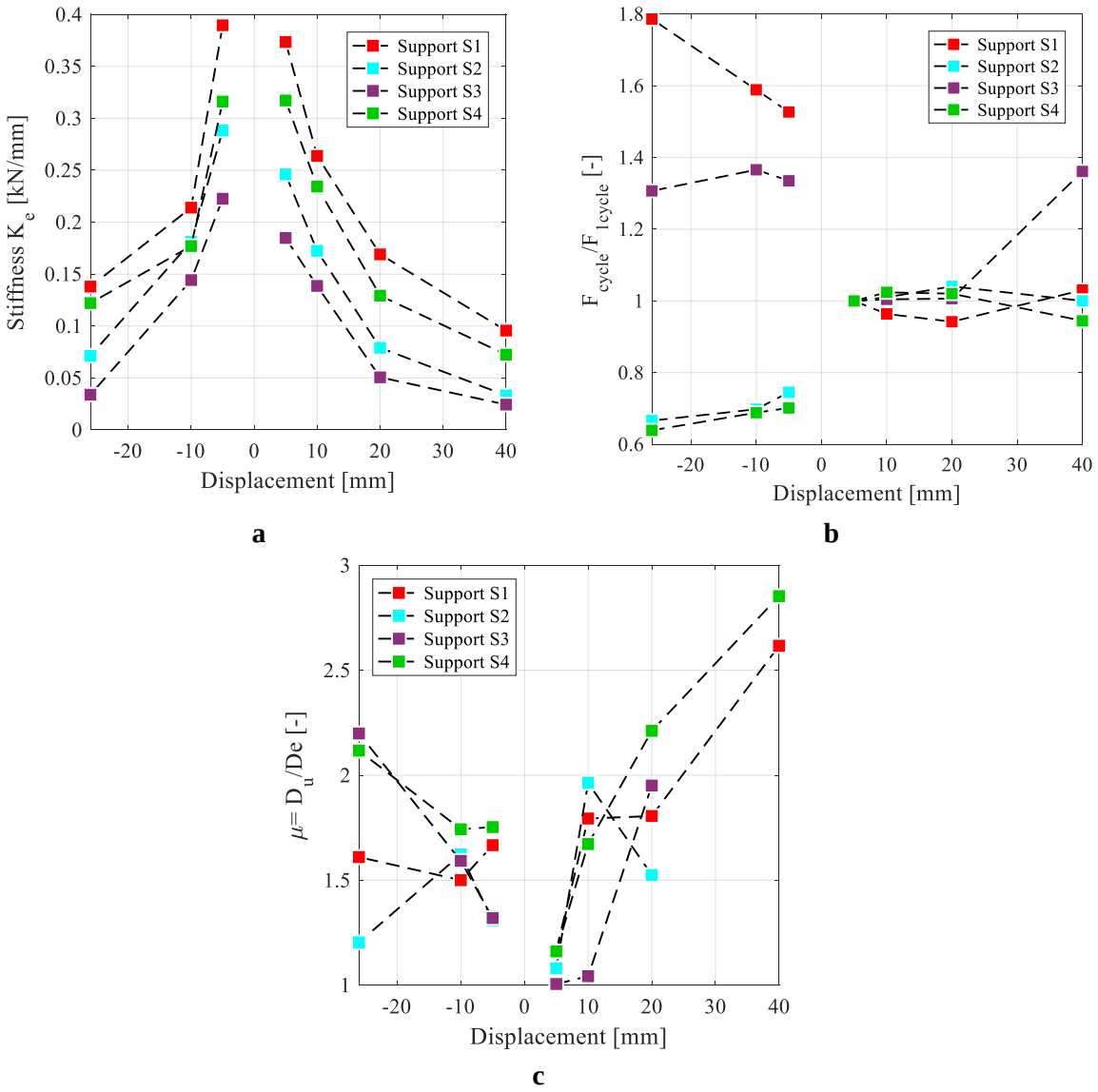

Figure 12: Experimental results: stiffness degradation depending on the displacement imposed (a), strength degradation (b) and ratio between the ultimate displacement in each cycle and the elastic one (c).

The load-displacement envelopes are shown in Figure 13 for all the supports monitored during the test. The first linear elastic phase is present at the beginning of the test. As confirmed by the visual inspection during this phase, no damage had occurred. The behaviour of the vault within the elastic branch was quite symmetric. However, a slight difference was found in their threshold values (5 mm and -3 mm). After cracking, the vault behaviour changed significantly. When upward displacements were applied, the trend of the reaction forces beyond the elastic phase was characterized by increasing values until reaching approximately a displacement of -10 mm. Although the results of S2 and S4 were more consistent with those of S1 and S3, all the supports showed a sudden drop in the vertical force of around

-10 mm. After this phase, strength gradually degraded in supports S4 and S2, as confirmed in Figure 12-b. Support S3 experienced a fairly constant trend in the vertical force, while it continued to increase in S1 until the test was stopped (Figure 12-b).

The behaviour of the vault when downward displacements were applied was quite different from the upward case. In almost all the supports the vertical force reached the peak load at approximately 15-20 mm. When the displacement reached 20 mm, the reaction load suddenly dropped and the strength rapidly degraded. Around 20 mm, a crack appeared along one of the diagonal elliptic arches which separated the vault into two independent parts. The displacement at failure increased by 25% with respect to the elastic limit, which partially confirmed one of the most important features of masonry cross vaults: their capacity to withstand movements of the supports. Several case studies in the technical literature [10] confirm that they frequently exhibit a significantly higher capacity to sustain vertical support displacement than horizontal movements.

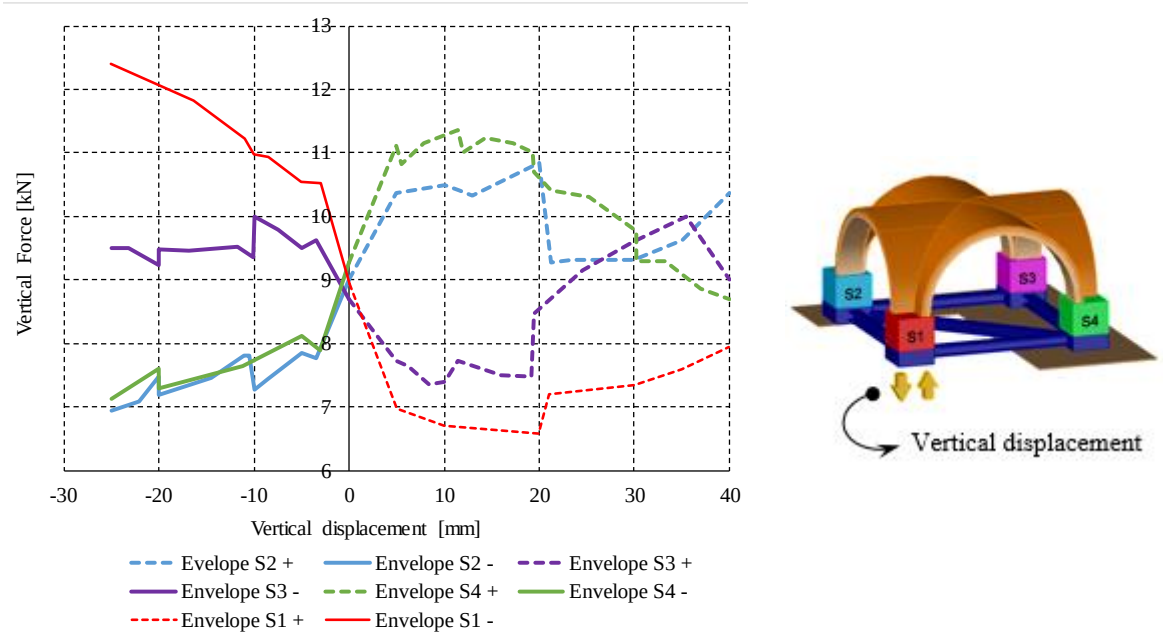

Figure 13: Experimental envelopes of maximum values of the force-displacement curves obtained for the four monitored supports.

5. Analysis of the results

This section is structured as follows: in Section 5.1 the crack development is analysed with respect to the settlement cycles and Section 5.2 analyses the structural behaviour of the vault.

5.1 Crack development

Visual inspections of the cross vault during the tests made it possible to evaluate the complex cracking phenomenon which took place. In the present work positive and negative values are used to identify downward and upward displacements, respectively (see Figure 5). As seen in Figure 13, the first linear elastic phase is present in the first and second cycles (i.e. from 5 to -3 mm). This phase is characterised by the absence of cracks and damage to the vault. Close to the end of the second cycle (at approximately -3 mm) some cracks became visible, as can be seen in Figure 14, in the form of flexural cracks in the two arches supported by S1 around an upward displacement of -3 mm and widened until the displacement reached -5 mm.

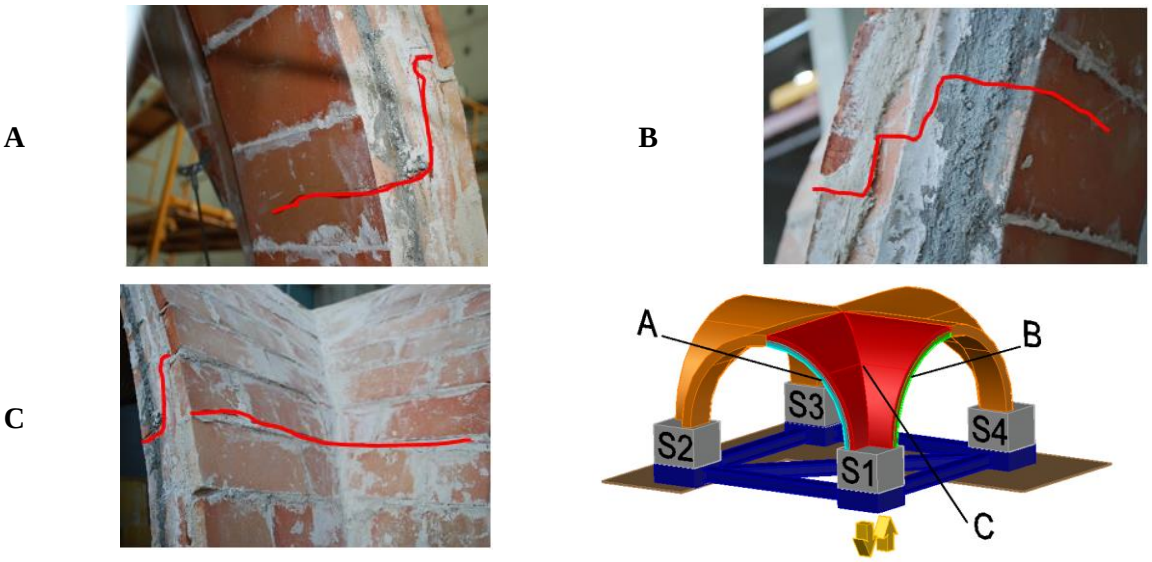

Figure 14: Cracks found in the arches close to the support S1.

The displacement was then reduced until reaching the starting point (position zero) and was increased to 10 mm in the third cycle. In the interval from 5 to 10 mm, some small damage was found in both the arches resting on support S2 (see Figure 15). The cracking phase described here was confirmed by the value of the vertical reaction monitored in this support. In the same interval, the trend of the vertical reaction force is approximately constant, which suggests the presence of a cracking mechanism.

A

B

Figure 15: Flexural cracks widened in the arches close to the support S2.

At around 10 mm, horizontal cracks formed in support S3, suggesting a tensile failure (see Figure 16-B).

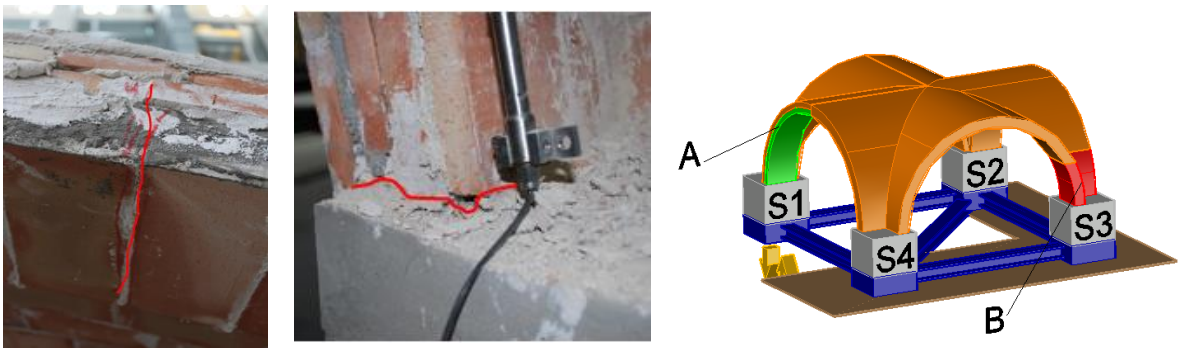

A **B**

Figure 16: Cracks found in the arch S1-S4 and in correspondence of the support S3.

The timbrel vault did not experience any apparent cracking mechanism during the interval from 10 mm to -10 mm (third-fourth cycles). When the displacement reached the value of -10 mm, two cracks suddenly developed along the diagonal elliptic arches. The intrados of the vault suffered a damage mechanism along the diagonal from support S1 to S4, which led to a sudden increase of the vertical reaction in S2. Conversely, another crack widened along the opposite diagonal (S2 to S3) and caused an abrupt drop of the vertical reaction in S3. The two cracking phenomena are depicted in Figure 17.

A **B**

Figure 17: Cracking mechanism along the two diagonals of the timbrel vault.

During the fifth cycle, at approximately 20 mm, flexural cracks occurred at -10 mm in the arch S1-S2 close to S2 and widened. The uncontrolled crack growth produced a sudden drop in the vertical reaction in the same support (S2), as confirmed by the experimental envelope curve depicted in Figure 13. From 5 mm to 20 mm, some cracks narrowed without closing completely. This effect is shown by the S2 envelope curve (Figure 13). In the same interval the reaction force is constant until reaching 20 mm. Up to this stage, the cracks opened mainly along the mortar joints, which were the weakest points in the structure. At a displacement of 20 mm, some cracks also appeared in the bricks. Finally, around -20 mm arches S1-S2 and S3-S4 experienced the formation of flexural cracks, as shown in Figure 16-A and at 20 mm a series of cracking patterns occurred. A crack widened along the diagonal elliptic arch S2-S4 on the upper vault surface (see Figure 18). At this point, the vault separated into two independent parts and its behaviour suddenly changed. The forthcoming failure was confirmed by the reduced vertical reaction forces in all the monitored supports. The final crack width along the diagonal elliptic arch was 8.2 mm.

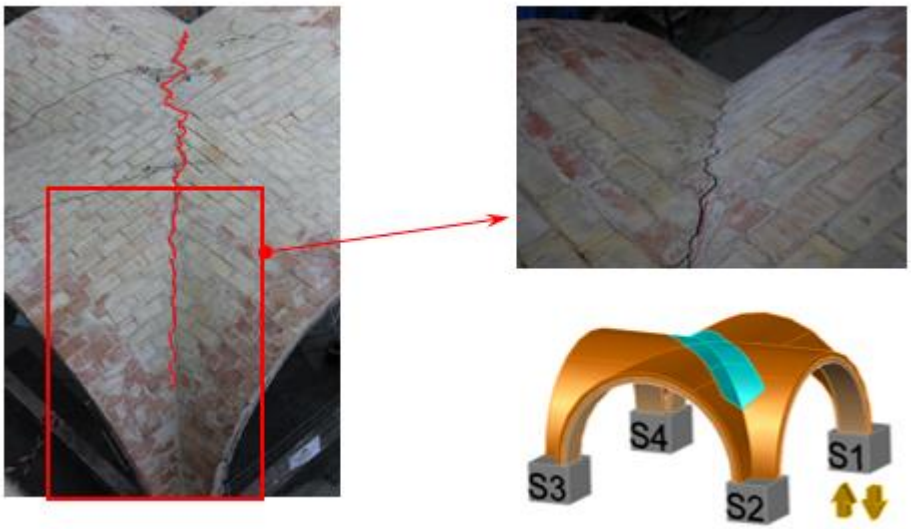

Figure 18: Diagonal crack along the elliptic arch S2-S4.

5.2 Structural behaviour

The behaviour of the cross vault is analysed here with respect to the history of displacements recorded during the test. The evolution of the displacements monitored by the sensors on the top of the cross vault is shown in Figure 19-a. All the LVDTs and FOSs were placed on elliptic arch S2-S4, the diagonal along which the failure was expected. All the sensors on the web extrados recorded similar values. The web extrados experienced the formation of a deep crack along the diagonal on which the sensors were placed in the last cycle at 20 mm. This crack, which affected the integrity of the vault, was detected by all the sensors. Different crack widths were recorded at different points by the LVDTs and FOSs. As expected, LVDT 7, at the intersection of the groins, detected the maximum value. The crack opening values ranged from 5 to 8.2 mm.

a

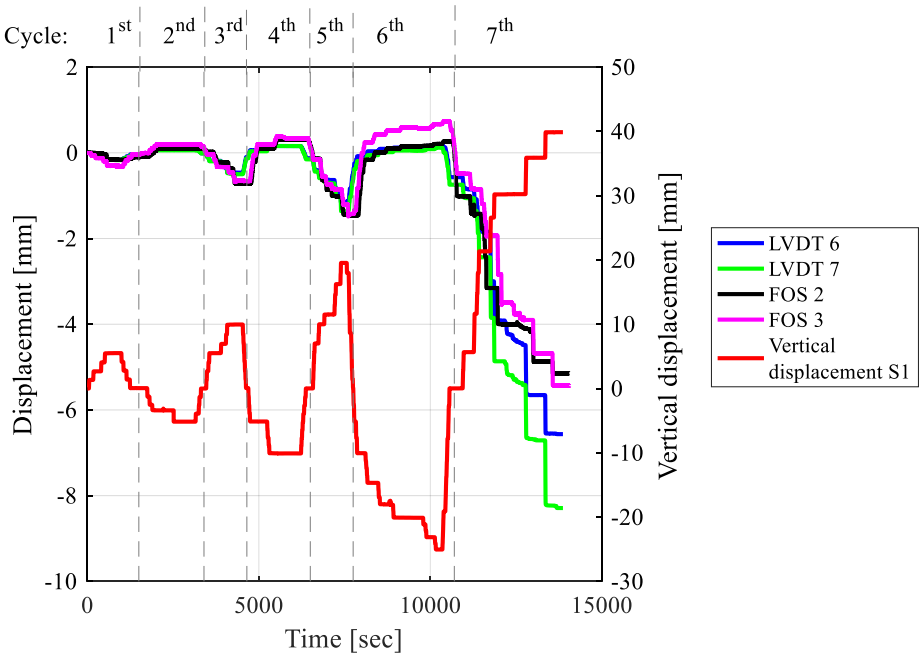

b

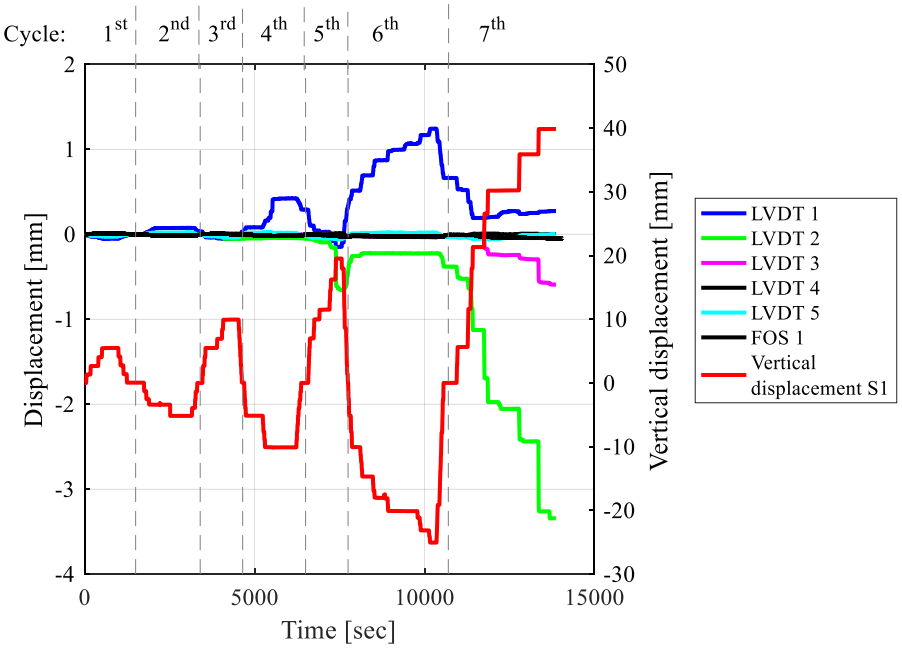

Figure 19: Displacement of the timbrel vault: (a) evolution of the displacements on the upper face of the masonry web and as recorded by other sensors (b).

In Figure 19-b, the time evolutions of the sensors placed close to the supports (LVDT 1 - LVDT 4 – FOS 1) and on the lateral arches (LVDT 2 – LVDT 3 – LVDT 5) are shown with respect to the displacement applied to S1. LVDT 2 recorded the maximum displacement value, approximately -3.5 mm (Figure 15-A). Arch S1-S2 experienced a series of cracking mechanisms in the fourth and fifth cycles, then closed, re-opened in the third, then narrowed again without closing completely (Figure 19-

b), and finally reached their maximum opening value in the last cycle. The maximum positive displacement was detected by LVDT 1, close to support S1 on the intrados of the vault. Support S1 was affected by several cracking mechanisms on its upper and lower surfaces (Figure 14-C). The displacement of approximately 1.2 mm occurred during the fifth and sixth cycles by the tensile failure of support S1. A crack widened across the sensor when the upward displacement reached -20 mm. This crack did not close completely during the last settlement cycle, as shown in Figure 19-b.

6. Conclusions

This paper describes a study of the behaviour of a masonry timbrel vault subjected to cyclic settlements carried out at one of ICITECH's laboratories at the *Universitat Politecnica de Valencia* (Spain) based on the cross vaults in the Church of San Lorenzo de Castell de Cabres (Castellón, Spain). The experimental set-up was designed to apply a series of displacement-controlled settlements to one of the vault supports (S1). During the test, a total of 23 sensors (Linear Displacement Transducers, Strain Gauges and Fibre Optic Sensors) were used to determine the vault behaviour. The overall behaviour of the masonry structure was described in terms of: (i) the reaction load-displacement curves of all the vault's supports, (ii) the experimental envelopes calculated from the load-displacement curves, (iii) the cracking patterns obtained in different time steps of the test, and (iv) the displacements detected by the LVDT and FO sensors fitted to the vault. As expected, the lateral arches experienced a series of flexural cracking mechanisms, while supports S1 and S3 were affected by tensile cracks. The failure of the vault was due to the widening of a crack along the diagonal elliptic arch S2-S4. The LVDTs placed near the groin intersection detected this crack's maximum opening value, which was 8.2 mm. The elastic stiffness recorded in support S1during the last cycle degraded approximately 30% with respect to the initial stiffness. A similar trend was detected in all the supports monitored. The maximum forces evolved differently according to the displacement imposed (i.e. upward/downward) and to the support analysed. Strength degradation was encountered only when upward displacements were imposed and not in all supports. When the vault was subjected to downward displacements, the vertical reactions remained quite constant till the end of the test. Conversely, the maximum ultimate displacement recorded during the test was equal to approximately three times the elastic displacement, considering

supports S1 and S4. This finding partially confirmed the results found in the technical literature on the collapse of masonry cross vaults. Indeed, several studies confirm that the displacement value at collapse is strongly influenced by the capacity of masonry cross vaults to withstand vertical movements of the supports better than horizontal displacements.

Since the technical literature lacks any reports on experimental tests on full scale masonry cross vaults, we consider this investigation an important step forward in the knowledge of the structural behaviour of this kind of masonry structure. However, additional work is still required and will involve the study of the behaviour of TRM/FRCM reinforced masonries subjected to monotonically increased displacement as well as cyclical movements.

Acknowledgments

The authors wish to express their gratitude to the Spanish Ministry of Economy, Industry and Competitiveness for the funding provided through Project BIA 2014-59036-R, and also to *LIC-Levantina Ingeniería y Construcción* and the *Grupo Puma* for their invaluable assistance.

The second author (Elisa Bertolesi) would like to thank the *Universitat Politècnica de València* for funding received for her postdoctoral grant (PAID-10-17).

References

[1] Bertolesi E, Adam JM, Rinaudo P, Calderón PA. Research and practice on masonry cross vaults – A review. Eng Struct 2019;180:67–88. doi:10.1016/j.engstruct.2018.10.085.

[2] Huerta Fernández S. The Debate about the Structural Behaviour of Gothic Vaults: From Viollet-le-Duc to Heyman. Proc Third Int Congr Constr Hist Brand Univ Technol Cottbus, Ger 20th-24th May 2009 2009:1558. doi:978-3-936033-31-1.

[3] D'Altri AM, Castellazzi G, de Miranda S, Tralli A. Seismic-induced damage in historical masonry vaults: A case-study in the 2012 Emilia earthquake-stricken area. J Build Eng 2017;13:224–43. doi:10.1016/j.jobe.2017.08.005.

[4] Compán V, Pachón P, Cámara M, Lourenço PB, Sáez A. Structural safety assessment of

geometrically complex masonry vaults by non-linear analysis. The Chapel of the Würzburg Residence (Germany). Eng Struct 2017;140:1–13. doi:10.1016/j.engstruct.2017.03.002.

[5] Núñez-Andrés MA, Buill F, Costa-Jover A, Puche JM. Structural assessment of the Roman wall and vaults of the cloister of Tarragona Cathedral. J Build Eng 2017;13:77–86. doi:10.1016/j.jobe.2017.07.007.

[6] Gaetani A, Lourenço PB, Monti G, Milani G. A parametric investigation on the seismic capacity of masonry cross vaults. Eng Struct 2017;148:686–703. doi:10.1016/j.engstruct.2017.07.013.

[7] Theodossopoulos D, Sinha BP, Usmani AS, Macdonald AJ. Assessment of the structural response of masonry cross vaults. Strain 2002;38:119–27. doi:10.1046/j.0039-2103.2002.00021.x.

[8] Theodossopoulos D, Sinha BP, Usmani a. S. Case Study of the Failure of a Cross Vault: Church of Holyrood Abbey. J Archit Eng 2003;9:109–17. doi:10.1061/(ASCE)1076-0431(2003)9:3(109).

[9] Croci G. General methodology for the structural restoration of historic buildings: The cases of the Tower of Pisa and the Basilica of Assisi. J Cult Herit 2000;1:7–18. doi:10.1016/S1296-2074(99)00119-3.

[10] Foti D, Vacca V, Facchini I. DEM modeling and experimental analysis of the static behavior of a dry-joints masonry cross vaults. Constr Build Mater 2018;170:111–20. doi:10.1016/j.conbuildmat.2018.02.202.

[11] Milani G, Rossi M, Calderini C, Lagomarsino S. Tilting plane tests on a small-scale masonry cross vault: Experimental results and numerical simulations through a heterogeneous approach. Eng Struct 2016;123:300–12. doi:10.1016/j.engstruct.2016.05.017.

[12] Rossi M, Calderini C, Lagomarsino S. Experimental testing of the seismic in-plane displacement capacity of masonry cross vaults through a scale model. Bull Earthq Eng

2016;14:261–81. doi:10.1007/s10518-015-9815-1.

[13] Atamturktur S, Bornn L, Hemez F. Vibration characteristics of vaulted masonry monuments undergoing differential support settlement. Eng Struct 2011;33:2472–84. doi:10.1016/j.engstruct.2011.04.020.

[14] Yardim Y, Mustafaraj E. Effects of soil settlement and deformed geometry on a historical structure. Nat Hazards Earth Syst Sci 2015;15:1051–9. doi:10.5194/nhess-15-1051-2015.

[15] Foraboschi P. Specific structural mechanics that underpinned the construction of Venice and dictated Venetian architecture. Eng Fail Anal 2017;78:169–95. doi:10.1016/j.engfailanal.2017.03.004.

[16] C. Valore, M. Ziccarelli. The preservation of Agrigento Cathedral. In: Proc of the 18th Int. Conf. on Soil Mechanics and Geotechnical Engineering, 2–6 2013, Paris. p. 3141–44. n.d.

[17] G. Cardani, D. Coronelli, G. Angjeliu. Damage observation and settlement mechanisms in the naves of the Cathedral of Milan. In: Proc. of 10th Int. Conf. on Structural Analysis of Historical Constructions (SAHC 2016), 13–15 September 2016, Leuven, Belgium. n.d.

[18] Portioli F, Cascini L. Large displacement analysis of dry-jointed masonry structures subjected to settlements using rigid block modelling. Eng Struct 2017;148:485–96. doi:10.1016/j.engstruct.2017.06.073.

[19] Acikgoz S, Soga K, Woodhams J. Evaluation of the response of a vaulted masonry structure to differential settlements using point cloud data and limit analyses. Constr Build Mater 2017;150:916–31. doi:10.1016/j.conbuildmat.2017.05.075.

[20] B. Sáez Riquelme. Iglesias Salón Valencianas del S. XVIII. Levantamiento gráfico, análisis geométrico y constructivo, patología común. PhD Thesis. Departamento de Sistemas Industriales y Diseño. Universitat Jaume I, Castellón (Spain), 2013. n.d.

[21] Gaetani A, Monti G, Lourenço PB, Marcari G. Design and Analysis of Cross Vaults Along History. Int J Archit Herit 2016. doi:10.1080/15583058.2015.1132020.

[22] Lusas 2010 Lusas Reference Manual (Surrey, UK: Lusas). n.d.

[23] Torres B, Payá-Zaforteza Ignacio I, Calderón PA, Adam JM. Analysis of the strain transfer in a new FBG sensor for Structural Health Monitoring. Eng Struct 2011;33:539–48. doi:10.1016/j.engstruct.2010.11.012.

[24] Górriz BT, García PC, Payá-Zaforteza IJ, Maicas SS. Experimental and numerical analysis of a hybrid FBG long gauge sensor for structural health monitoring. Meas Sci Technol 2014;25. doi:10.1088/0957-0233/25/12/125107.

[25] https://www.hbm.com/es/2290/software-adquisicion-de-datos-catman/. Accesed on 11th April, 2018. n.d.

[26] http://www.micronoptics.com/products/sensing-solutions/software/. Accesed on 11th April, 2018. n.d.